Journal of Applied Polymer Science

Microstructural Design of Lead Oxide–Epoxy Composites for Radiation Shielding Purposes

Nurul Zahirah Noor Azman,[1,2] Salim Ahmed Siddiqui,[1] Robin Hart,[3] It Meng Low[1]

[1]Department of Imaging and Applied Physics, Faculty of Science and Engineering, Curtin University, Perth, Western Australia 6845, Australia

[2]School of Physics, Universiti Sains Malaysia, 11800 Penang, Malaysia

[3]Department of Radiology, Royal Perth Hospital, East Perth, Western Australia 6001, Australia

Correspondence to: I. M. Low (E-mail: j.low@curtin.edu.au)

ABSTRACT: Composite epoxy samples filled with PbO and Pb3O4 were fabricated to investigate the mass attenuation characteristics of the composites to X-rays in the diagnostic imaging energy range. The effect of density on the attenuation ability of the composites for radiation shielding purposes was studied using a calibrated X-ray machine. Characterization of the microstructure properties of the synthesized composites was performed using synchrotron radiation diffraction, optical microscopy, and scanning electron microscopy. The results indicate that the attenuation ability of the composites increased with an increase in density. The particle size of WO_3 fillers has a negligible effect on the value of mass attenuation coefficient. Microstructural analyses have confirmed the existence of fairly uniform dispersion of fillers within the matrix of epoxy matrix with the average particle size of 1–5 μm for composites with filler loading of $\leq$ 30 wt % and 5–15 μm for composites with filler loading of $\geq$ 50 wt %. © 2012 Wiley Periodicals, Inc. J. Appl. Polym. Sci. 000: 000–000, 2012

KEYWORDS: radiation; radiation shielding; resins; composites; density; microscopy

Received 25 June 2012; accepted 25 August 2012; published online
DOI: 10.1002/app.38515

INTRODUCTION

During the early part of the 20th century, the hazards from ionizing radiation were recognized, and the use of lead and other materials became commonplace for shielding against X-rays.[1–3] Once the dangers of X-rays are considered, lead has become an important material for radiation protection. Since then protection has evolved into an elaborate infrastructure of controls and disciplines specifying how this shield should be deployed.[4–6] Recently, shielding requirements have become more stringent as standards for exposure of personnel and the general public. X-ray technologists practice a principle called as-low-as-reasonably-achievable dose when dealing with X-rays, so that radiation dose received by personnel and the general public can be as low as possible.[3,7]

The shielding for radiation purposes are based on the type and energy of the radiation itself. Gamma and X-rays are the most penetrating radiations as compared to other ionizing radiations. Their interaction depends on the probability of their collision with the atoms of the materials during the interaction. To increase the probability, they will interact the density of the material they are passing through needs to be increased which means the materials should have a lot of atoms with an assumption that the materials are free from voids. If dealing with a material having a lot of pores, porosity needs to be taken into account, because it will affect the interaction of the radiations with the atoms within the material.[8]

Lead-glass is one example of the material used as shielding materials for ionizing radiations, but it is heavy, expensive, and very brittle. So, it is not surprising that polymers have made inroads into markets that were in the beginning dominated by glass. Polymers also have a great potential in many important applications that glass could not meet because of their unique properties, such as a low density, ability to form intricate shapes, optical transparency, low manufacturing cost, and toughness. However, the use of polymers is still limited, because of their inherent softness and low thermal stability.[9,10] One modern example of the filler-reinforced polymer used for radiation shielding is lead-acrylic.[11,12] Moreover, many researchers tried to create new lead-based composites for this radiation shielding purposes such as lead-polyester composites,[13] lead-styrene butadiene rubber,[14] lead-polystyrene,[15] and similar materials.

Table I. List of Composites Prepared with Different Weight Fractions of Filler and Epoxy System and Corresponding Designations Used in This Study

Composite by weight fraction (wt %)			Composite designation
Filler		Epoxy system	
PbO	10	90	A1
	30	70	A2
	50	50	A3
	70	30	A4
Pb_3O_4	10	90	B1
	30	70	B2
	50	50	B3
	70	30	B4

Rudraswamy et al.[16] have shown that some lead compounds such as PbO, PbO_2, $PbNO_3$, and $PbCl_2$ have an adequate mass attenuation coefficient, μ_m for use in radiation shielding purposes. Unfortunately, the usage of either lead or lead compounds alone will cause certain health risks to human, animals, and also to the surroundings.[17] Moreover, lead or lead compounds themselves are also not really malleable and lack in mechanical strength.[18]

Additionally, there are many methods available to achieve a good dispersion of fillers within a polymeric matrix. One of the traditional methods for dispersing fillers in polymer matrices is melt-mixing method of the fillers into the polymer. The fillers are weighted and added straightly into the polymer for mixing. In many works done, many researchers used a static mixer with constant speed during the mixing process to achieve homogenously dispersion of fillers within the polymers.[13,19]

It is expected that lead oxide–epoxy composites will be a good material to be used as radiation shielding in diagnostic radiology purposes. This is because lead oxide can be easily dispersed within a polymer matrix.[13] Besides, an epoxy system is a thermoset material that is generally stronger and better suited to higher temperatures than thermoplastics, so it can withstand the high energetic X-rays bombardment during the diagnostic imaging.[20] Hence, the purpose of this study is to prepare and characterize a composite that is made of an epoxy system filled with lead oxides. The feasibility of this material for use in X-ray shielding is discussed.

EXPERIMENTAL METHODS

Samples Preparation

To prepare PbO–epoxy composite samples, micron-sized PbO powder (Chem Supply, Gillman, South Australia, product number LL021) was added into the FR251 epoxy resin (Bisphenol-A diglycidyl ether polymer) before the FR251 hardener (isophoronediamine) was mixed into it. The ratio of epoxy resin to hardener used was 2 : 1. The mixing of PbO powder in epoxy resin was done through gentle stirring with a wooden stick within a beaker with constant speed for 10 min to ensure fairly uniform dispersion of the powder in epoxy matrix. The well-mixed mixture was then cast in a 4 × 6 cm^2 rectangular silicon rubber mold with a thickness of 5 mm and was allowed to set overnight at room temperature. The list of samples with different weight percentages of PbO are shown in Table I.

The same procedure was used to prepare epoxy composites filled with micron-sized Pb_3O_4 powder (Chem Supply, Gillman, South Australia, product number LL027). The list of samples is also shown in Table I.

Density Measurements

The apparent density ρ of prepared samples was measured using the Archimedes method and calculated using eq. (1).[21] A calibrated single pan electrical balance, ethanol, and toluene were used for this purpose.

$$\rho = \frac{m_1}{m_2 - m_3}(\rho_l) \tag{1}$$

where m_1, m_2, and m_3 are the mass of the sample weighted on the balance, the mass of the sample hanging on balance arm in the air, and the mass of the sample hanging on the balance arm immersed in ethanol or toluene, respectively, whereas ρ_l is the density of the immersion liquid.

The measured densities were compared with the theoretical values, ρ_c (with an assumption that the samples were free from voids) which are determined according to eq. (2)[13]:

$$\rho_c = \frac{100}{\left[\frac{F}{\rho_f} + \frac{E}{\rho_e}\right]} \tag{2}$$

where F is the wt % of the filler, E is the wt % of epoxy, ρ_f is the density of filler, and ρ_e is the density of epoxy.

Measurement of X-Ray Mass Attenuation Coefficients

To determine the initial dose (D_o), the generated X-rays were directly exposed to the DIADOS diagnostic detector connected to DIADOS diagnostic dosemeter (PTW-Freiburg, Germany) without having passed though any sample. The distance between the X-ray tube and the detector was set to 100 cm, and the X-ray beam was well collimated according to the size of the sample. This experiment was done using a calibrated X-ray machine in Royal Perth Hospital, Western Australia. The final dose (D) was taken with the sample placed on the detector. The exposure was set at 10 mA s, where the X-ray tube voltage was started at 40 kV_p with 10 kV_p increment up to 100 kV_p. Next, the linear attenuation coefficient, μ, for each sample was determined by eq. (3), where x is the thickness of the sample. This μ is divided by the calculated ρ_c to determine μ_m [eq. (4)].

$$\mu = \frac{\left(\ln \frac{D_0}{D}\right)}{x} \tag{3}$$

The observed results of μ_m were compared with the theoretical values evaluated from Hubbell's database, NIST XCOM.

$$\mu_m = \frac{\mu}{\rho_c} \tag{4}$$

Powder Diffraction

Powder diffraction measurements were performed at the Australian Synchrotron in Melbourne to identify the crystalline phases

Table II. Comparison of Measured and Theoretical Density Values for the Composites

Composite designation	Density of composite, ρ_{comp} (g/cm^3)	
	Theoretical	Measured
A1	1.26	1.26 ± 0.01
A2	1.56	1.53 ± 0.01
A3	2.06	2.05 ± 0.02
A4	3.00	2.93 ± 0.03
B1	1.26	1.26 ± 0.01
B2	1.55	1.55 ± 0.01
B3	2.02	2.00 ± 0.03
B4	2.90	2.83 ± 0.03

present in the samples. This work was conducted on the Powder Diffraction beamline, and the diffraction patterns were recorded in the 2θ range of 10–60° at a fixed wavelength of 1.37 Å.

Optical Microscopy

Optical microscopy was done using Nikon ME600 optical microscope. The samples were polished using diamond pastes from 15 to 1.0 μm to obtain mirror-like surface finish.

Scanning Electron Microscopy

The surface of the samples was also examined using a Zeiss Evo 40XVP scanning electron microscope. Samples were Pt-coated to prevent any charging on the samples during the imaging process. The backscattered electron technique was chosen to gain better contrast because of different atomic number between epoxy and lead. A pure epoxy sample was also examined as a control.

Table III. Equivalent Energy for the Various X-Ray Tube Voltages Used

X-ray tube voltage (kV$_p$)	Equivalent energy (keV)
40	29.9
50	34.3
60	38.5
70	42.5
80	46.2
90	49.7
100	52.9

RESULTS AND DISCUSSION

Density of Samples

As can be seen from Table II, the values of apparent density for samples obtained from the Archimedes' technique did not totally agreed with the theoretical values because of experimental uncertainties. The porosity calculated for each sample was less than 1%. Besides, the higher the wt % of the filler within the composite, the higher the value of ρ_c as also been observed by Harish et al.[13,22]

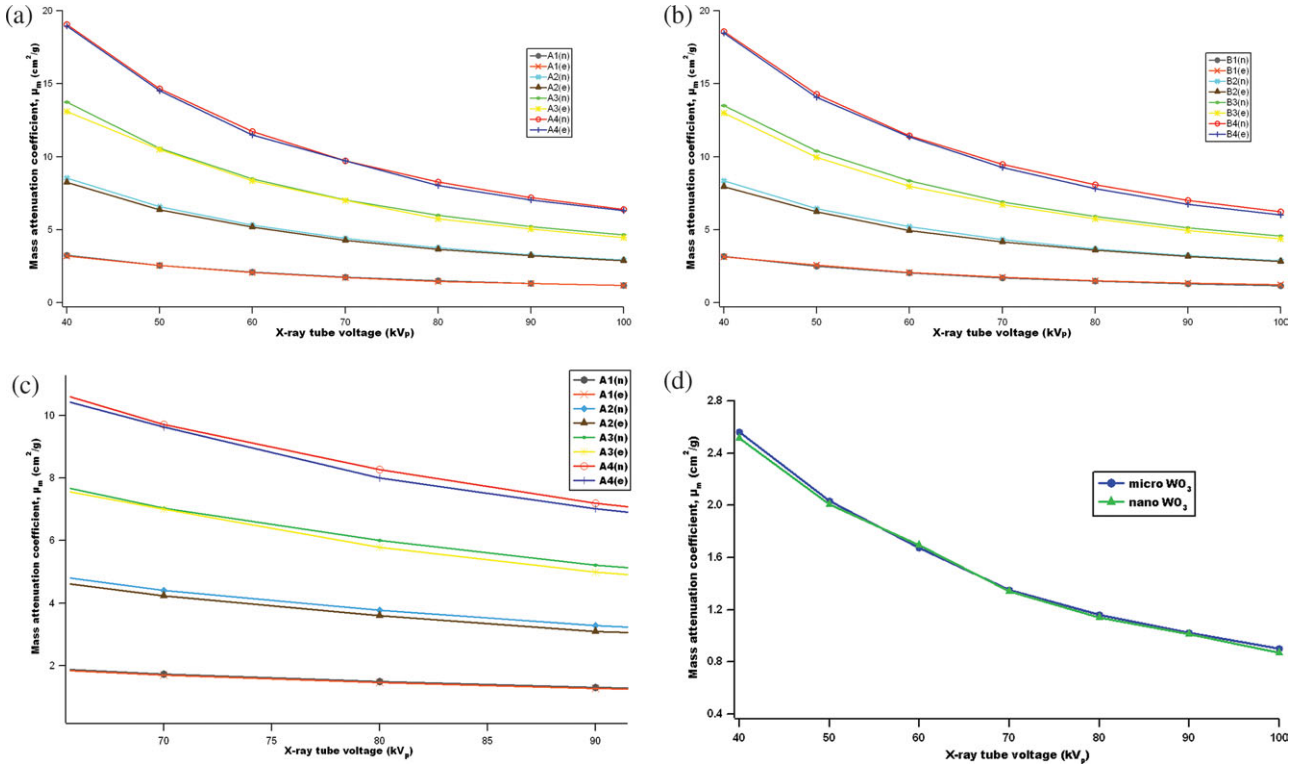

Figure 1. Mass attenuation coefficients as a function of kV$_p$ as obtained from NIST (n) and experiment (e) for samples of (a) PbO–epoxy composite, (b) Pb3O4–epoxy composite, (c) close-up view of (a), and (d) micro- and nano-WO3 epoxy composites. [Color figure can be viewed in the online issue, which is available at wileyonlinelibrary.com.]

Table IV. Mass Attenuation Coefficients Interpolated from NIST Databases for Gamma Rays of Energy 0.662 MeV from Cs-137 Point Source

Composite designation	Mass attenuation coefficient, μ_m (cm^2/g)
A1	0.0871
A2	0.0924
A3	0.0978
A4	0.1055
B1	0.0871
B2	0.0922
B3	0.0974
B4	0.1025

X-Ray Mass Attenuation Coefficients

The μ_m values given in NIST are specifically measured for characteristic photon energy, whereas in this experiment; the X-ray tube voltages used are in continuous spectrum. So, the equivalent energies for the X-ray tube voltages used within the experiment must be taken into account for comparing the value of μ_m between NIST and experiment. The equivalent energies for the X-rays tube voltages used are shown in Table III. These values were calculated using the equation fitted as an exponential function[23]:

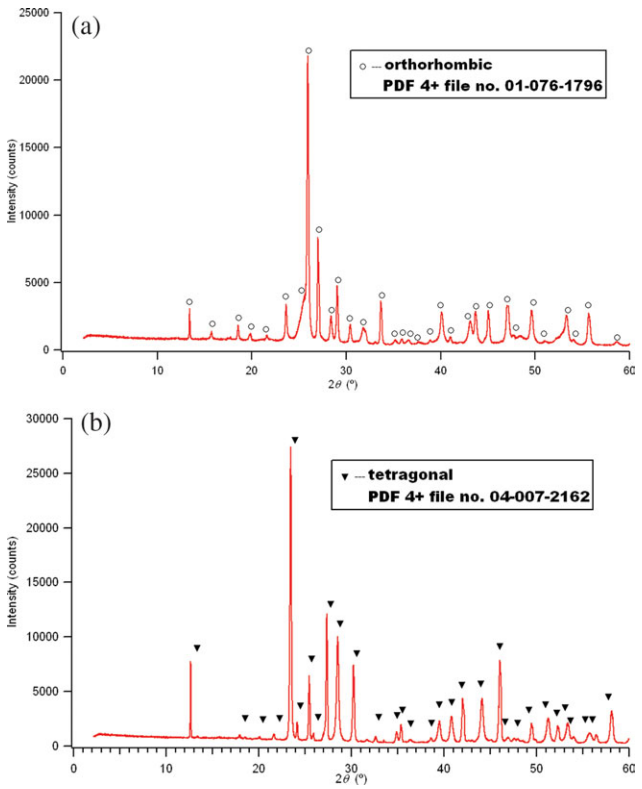

Figure 2. Typical powder diffraction patterns for (a) PbO–epoxy composite and (b) Pb3O4–epoxy composite. [Color figure can be viewed in the online issue, which is available at wileyonlinelibrary.com.]

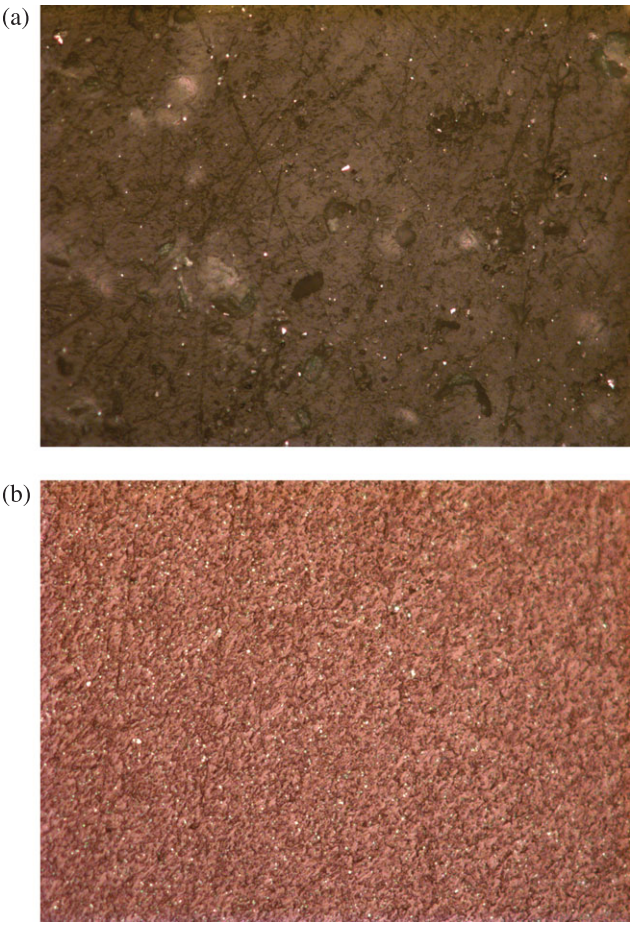

Figure 3. Optical micrographs showing the typical uniform dispersion of fillers in the matrix of epoxy for two composite samples: (a) A3 and (b) B2. 50 × magnification. [Color figure can be viewed in the online issue, which is available at wileyonlinelibrary.com.]

$$y = a_{\exp}^{-\left(\frac{x}{c}\right)} + b \tag{5}$$

where a, b, and c in the eq. (5) are constants with values of −97.535, 106.857, and 168.672, respectively, whereas y is the equivalent energy and x is the X-ray tube voltage.

For composites, the value of μ_m was calculated using eq. (6):

$$\mu_m = \sum w_i \mu_{m_i} \tag{6}$$

where μ_m is the mass attenuation coefficient of the composite, whereas w_i and μ_{m_i} are the weight fraction and the mass attenuation coefficient of each compound used to make the composite, respectively.

The plots in Figure 1(a–c) show that almost all the lines for the μm experimental values were a few percent lower than the μ_m values interpolated from NIST for the given X-ray tube voltages. These results are similar to the work done by Gerward et al., which they have found that tabulated X-ray mass attenuation coefficients are commonly a few percent higher than the measured values.[24,25] Içelli et al.[26] obtained very similar results

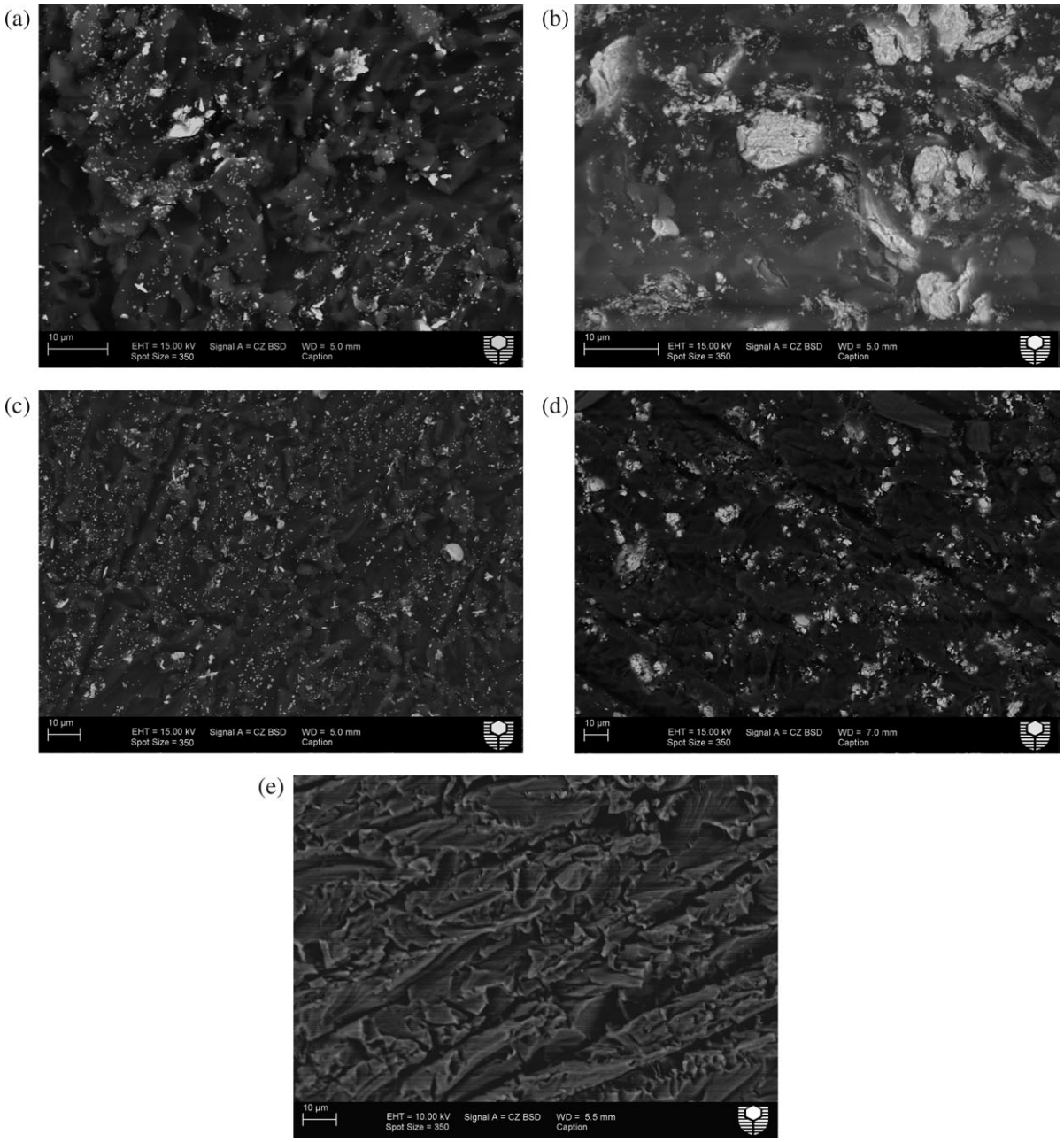

Figure 4. SEM micrographs showing the uniform dispersion of PbO or Pb3O4 particles within the epoxy matrix in various composite samples: (a) A3, (b) A4, (c) B2, (d) B3, and (e) pure epoxy.

where the higher the density of the material, the higher the value of μ_m.

However, the relationship between mass attenuation coefficient (μ_m) and particle size of lead oxide remains unknown. In particular, would the use of nanosized lead oxide increase or decrease the value of μ_m? As nanosized lead oxide was not available, the effect of particle size of WO_3 filler (purchased from Sigma–Aldrich, Castle Hill, NSW, Australia) on μ_m was studied. The procedure to prepare this composite was similar to that for preparing PbO–epoxy samples. Figure 1(d) shows the effect of particle size on the mass attenuation coefficient in epoxy composite filled with either microsized ($\sim$20 μm) or nanosized ($<$100 nm) WO_3. It is clearly shown that particle size has a negligible effect on the value of μ_m of a material for this range of X-ray energy 40–100 kV_p. However, it should be noted that nanosized particles (e.g., CuO) have been reported to show better X-ray attenuation at the lower X-ray beam energy (i.e., 26–30 kV).[27,28] As photoelectric absorption dominates at low photon energies, the probability of an X-ray with low energy to interact and to be absorbed is higher for nanosized particles, in addition to maximization of the surface/volume ratio. However, as photon energy increases, the probability of Compton scattering increases, and hence the attenuation by the material decreases, as this interaction is weakly dependent on atomic

number of the element and the photon energy. Hence, the probability of an X-ray with higher energy to interact and to be absorbed becomes similar for both nanosized and microsized particles. It appears that the use of nanosized particles only helps in providing a fairly uniform dispersion within the epoxy matrix but has no direct effect on the value of μ_m as clearly indicated in eq. (4). Only the abundance of WO_3 dispersed in the composite will influence the value of μ_m.

The mass attenuation coefficient, μ_m is the rate of photon interactions within 1-unit of mass per 1-unit of area (g/cm^2). It depends on the energy of the photon and the concentration of electrons in the material. Its value will decrease rapidly with the increment of photon energy. Further the chance of a photon coming close enough to an electron is higher when the concentration of electrons within the material is higher, because it is absorbed by the material. Electron concentration was determined by the physical density of the material. Thus, composites with a fine dispersion of high density material provide more interaction probability for photons and also better radiations shielding properties.[13,29]

To ascertain the shielding ability of the composites, calculations of $\mu\mu_m$ were done to compare the 50 wt % of PbO reinforced isophthalate resin composite performed by Harish et al.[13] The value of μ_m for their composite was calculated to be 0.0948 cm^2/g, whereas the values of μ_m for samples A3 and B3 in this study, which also have 50 wt % of the fillers, were 0.0978 and 0.0974 cm^2/g, respectively. The calculation of μ_m was done by interpolating NIST databases for gamma rays of energy 0.662 MeV from a Cs-137 point source. These results show that samples A3 and B3 in this study provided better radiation shielding than the composite fabricated by Harish and coworkers. Moreover, the usage of lead oxides for radiation shielding can be minimal in the fabrication of composites and thus reduce the health risks associated with lead oxides. The results for other samples at the same energy range are shown in Table IV.

Phase Compositions

The reference for phase-fitting the peaks were taken from International Centre for Diffraction Data PDF−4 + 2009 database. The wavelength for all of these databases was chosen to be the same as the wavelength of the synchrotron radiation used.

From Figure 2(a), all the peaks belong to orthorhombic PbO crystal structures (PDF−4 + files 01-076-1796). While for composite filled with Pb3O4 powder, all the peaks were identified as tetragonal Pb3O4 crystal structures (PDF−4 + file 04-007-2162) as shown in Figure 2(b). These indicate that the powders of PbO and Pb3O4 used were single-phase pure.

Microstructures

The typical fracture surfaces for the samples are shown in Figure 3. The scratches seen in the images were due to the polishing process. These images have shown that the fractured surfaces were quite rough, and the fillers (white patches) were well dispersed and firmly embedded in the epoxy matrix due to their relatively small particle size and good compatibility with the epoxy matrix. Although the fillers have a greater weight fraction than epoxy, they were dispersed quite uniformly with only some agglomerations to be found. As can be seen in Figure 3(a), the blurry white patches are clear indications of some minor filler agglomerations.

The scanning electron microscopy (SEM) images in Figure 4 have provided results that agreed with the optical images shown in Figure 3. The bright regions represent the filler particles (lead-oxide) dispersed in the dark epoxy matrix. The fillers were seen to be quite uniformly dispersed in the composites, although minor agglomerations can be observed. The average particle size obtained from the SEM images was ~1–5 μm for composites with filler loading of $\leq$ 30 wt % and ~5–15 μm for composites with filler loading of $\geq$ 50 wt %.

CONCLUSIONS

Epoxy composites filled with fairly dispersed lead oxide particles of 1–5 μm for composites with filler loading of $\leq$ 30 wt % and 5–15 μm for composites with filler loading of $\geq$ 50 wt % have been successfully fabricated. These composites showed good X-ray attenuation properties and could be considered as a potential candidate for radiation shielding in diagnostic radiology purposes. The particle size of WO_3 fillers has a negligible effect on the value mass attenuation coefficient (μ_m) for the X-ray energy of 40–100 kV_p. In addition, the lead oxide–epoxy composites in this study are superior to the lead oxide-isophthalate resin composite previously investigated.

ACKNOWLEDGMENTS

The funding for the collection of synchrotron powder diffraction data at the Australian Synchrotron in this work was provided by Grant Number AS111/PD3509 and AS111_PDFI3181.

REFERENCES

1. Archer, B. R.; Thornby, J. I.; Bushong, S. C. *Health Phys.* **1983**, *44*, 507.
2. Archer, B. R. *Health Phys.* **1995** *69*, 750.
3. Archer, B. R. *Health Phys.* **2005**, *88*, 579.
4. Hessenbruch, A. *Endeavour* **2002**, *26*, 137.
5. Okunade, A. A. *Appl. Radiat. Isotopes* **2002**, *57*, 819.
6. Okunade, A. A. *Med. Phys.* **2004**, *31*, 513.
7. Dixon, R. L.; Simpkin, D. *J. Health Phys.* **1998**, *74*, 181.
8. Lorenzen, W. MadSci Network: Engineering, **2000**.
9. Polymer versus Glass, POLYMICRO Newsletter, 2004. Available at: http://www.polymicro-cc.com. Accessed on 24 June 2011.
10. Lee, E. H., Rao, G. R., Lewis, M. B., Mansur, L. K. *Nucl. Instrum. Methods Phys. Res. Sect. B: Beam Interact. Mater. Atoms* **1993**, *74*, 326.
11. Premac Lead Acrylic, Part of the Wardray Premise Total Radiation Shielding Package, Wardray Premise Ltd. Available at: http://wardray-premise.com/structural/materials/premac.html. Accessed on 4 May 2011.
12. Radiation Safety & Consumable Products. Available at: http://www.lablogic.com/moreinfo/PDF/consumables/lablogic_consumables_brochure.pdf. Accessed on 4 May 2011.

13. Harish, V.; Nagaiah, N.; Prabhu, T. N.; Varughese, K. T. *J. Appl. Polym. Sci.* **2009**, *112*, 1503.
14. Abdel-Aziz, M. M.; Badran, A. S.; Abdel-Hakem, A. A.; Helaly, F. M.; Moustafa, A. B. *J. Appl. Polym. Sci.* **1991**, *42*, 1073.
15. Pavlenko, V. I.; Lipkanskii, V. M.; Yastrebinskii, P. N. *J. Eng. Phys. Thermophys.* **2004**, *77*, 11.
16. Rudraswamy, B.; Dhananjaya, N.; Manjunatha, H. *Nucl. Instrum. Methods Phys. Res. Sect. A: Accelerators Spectrometers Detectors Associated Equipment* **2010**, *619*, 171.
17. Robert, R. D. High Density Composites Replace Lead; Ecomass Technologies, Austin, Texas, USA **2005**.
18. Spinks, J. W. T.; Wood, R. J. An Introduction to Radiation Chemistry, Wiley-Interscience: New York, **1976**.
19. Tanahashi, M. *Materials* **2010**, *3*, 1593.
20. Material Guide, Archos LLC. Available at: http://www.archos-llc.com/Material_Guide_2.html. Accessed on 20 June 2011.
21. Australian Standards 1774.5, Method 5. The Determination of Density, Porosity and Water Absorption, 1989.
22. Berger, M. J.; Hubbell, J. H.; Seltzer, S. M.; Chang, J.; Coursey, J. S.; Sukumar, R.; Zucker, D. S.; Olsen, K. XCOM: Photon Cross Section Database (version 1.5), National Institute of Standards and Technology, Gaithersburg, MD, **2010**. Available at: http://physics.nist.gov/xcom. Accessed on 20 June 2011.
23. Mincong, C.; Hongmei, L.; Ziyu, C.; Ji, S. *Appl. Radiat. Isotopes* **2008**, *66*, 1387.
24. Gerward, L. *Nuclear Inst. Methods Phys. Res. B* **1992**, *69*, 407.
25. Midgley, S. M. *Radiat. Phys. Chem.* **2005**, *72*, 525.
26. Içelli, O.; Erzeneoglu, S.; Boncukçuoglu, R. *Ann. Nuclear Energy* **2004**, *31*, 97.
27. Botelho, M. Z.; Künzel, R.; Okuno, E.; Levenhagen, R. S.; Basegio, T.; Bergmann, C. P. *Appl. Radiat. Isotopes* **2011**, *69*, 527.
28. Künzel, R.; Okuno, E. *Appl. Radiat. Isotopes* **2012**, *70*, 781.
29. Sprawls, P. The Physical Principles of Medical Imaging, Aspen Publishers: Gaithersburg, Md **1993**.